10-2020

Deep Donor Behavior of Iron in β-Ga_2O_3 Crystals: Establishing the $Fe^{4+/3+}$ Level

Timothy D. Gustafson
Air Force Institute of Technology

Christopher A. Lenyk
Air Force Institute of Technology

Larry E. Halliburton
West Virginia University

Nancy C. Giles
Air Force Institute of Technology

Journal of Applied Physics

Deep donor behavior of iron in β-Ga_2O_3 crystals: Establishing the $Fe^{4+/3+}$ level

Cite as: J. Appl. Phys. **128**, 145704 (2020); https://doi.org/10.1063/5.0021756
Submitted: 13 July 2020 • Accepted: 23 September 2020 • Published Online: 14 October 2020

T. D. Gustafson, C. A. Lenyk, L. E. Halliburton, et al.

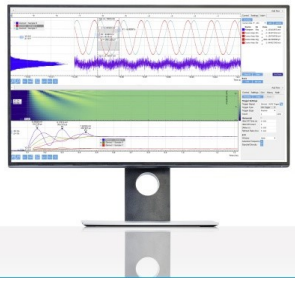

Journal of Applied Physics ARTICLE scitation.org/journal/jap

Deep donor behavior of iron in β-Ga_2O_3 crystals: Establishing the $Fe^{4+/3+}$ level

Cite as: J. Appl. Phys. **128**, 145704 (2020); doi: 10.1063/5.0021756
Submitted: 13 July 2020 · Accepted: 23 September 2020 ·
Published Online: 14 October 2020

View Online Export Citation CrossMark

T. D. Gustafson,[1,a)] C. A. Lenyk,[1] L. E. Halliburton,[2] and N. C. Giles[1,a)]

AFFILIATIONS

[1]Department of Engineering Physics, Air Force Institute of Technology, Wright-Patterson Air Force Base, Ohio 45433, USA
[2]Department of Physics and Astronomy, West Virginia University, Morgantown, West Virginia 26506, USA

[a)]**Authors to whom correspondence should be addressed:** timothy.gustafson@protonmail.com and nancy.giles@afit.edu

ABSTRACT

The $Fe^{4+/3+}$ donor level is experimentally determined to be 0.70 eV (±0.05 eV) above the valence band maximum in β-Ga_2O_3. Electron paramagnetic resonance (EPR) is used to monitor Fe^{3+} ions that are unintentionally present in an Mg-doped β-Ga_2O_3 crystal (with a low Fermi level). For temperatures near 255 K, exposure to 325 nm laser light converts a portion of the Fe^{3+} ions to Fe^{4+} and Fe^{2+} ions and, at the same time, forms neutral magnesium acceptors (Mg^0_{Ga}) and neutral Ir donors (Ir^{3+}). After removing the light, the intensity of the Fe^{3+} EPR spectrum has a significant additional decrease as holes thermally released to the valence band from rapidly decaying neutral Mg acceptors are trapped at Fe^{3+} ions and form even more Fe^{4+} ions. This demonstrates that the $Mg^{0/-}$ acceptor level, near 0.65 eV, is closer to the valence band than the $Fe^{4+/3+}$ level. Following the fast initial post-light decrease, the Fe^{3+} spectrum then slowly recovers as Fe^{4+} ions are destroyed by electrons thermally excited from the valence band. An activation energy for the thermal decay of the Fe^{4+} donors, and thus a value for the $Fe^{4+/3+}$ level, is obtained from the analysis of five Fe^{3+} isothermal recovery curves taken from the Mg-doped crystal between 250 and 270 K. A first-order kinetics model is used, as minimal retrapping is observed. In separate experiments, EPR shows that Fe^{4+} ions are also produced in an Fe-doped β-Ga_2O_3 crystal (without Mg acceptors) during exposures to laser light at temperatures near 255 K.

I. INTRODUCTION

Iron is an important impurity in β-Ga_2O_3 crystals. It is present at trace levels (10^{16}–10^{17} cm^{-3}) in nearly all bulk-grown crystals because of impure starting materials, and in recent years, it has become the dopant of choice to produce semi-insulating β-Ga_2O_3 substrates for use in thin film growth. With the goal of improving the performance of emerging devices, numerous studies have been made by various research groups to establish the optical and electrical properties of iron ions in this ultrawide-band-gap semiconductor.[1–20] Much of this attention has focused on the deep acceptor behavior of the Fe ions. The $Fe^{3+/2+}$ acceptor level, or (0/−) level in conventional semiconductor notation, is approximately 0.8 eV below the conduction band minimum,[2,8] thus allowing iron to provide compensation for the unintentional shallow donors that are typically present, such as Si, Ge, and Sn. Although not studied experimentally until now, iron also has a deep donor level in β-Ga_2O_3 crystals. The $Fe^{4+/3+}$ donor level, or (+/0) level, is expected to be in the lower half of the bandgap, with recent computational results predicting it to be 0.51 eV above the valence band maximum.[2,7] This ability of Fe to act as both a donor and an acceptor in β-Ga_2O_3 makes it an amphoteric defect.[21] Future investigations of Fe-doped material that monitor transient carrier trapping and retrapping may need to consider both types of behavior for this impurity.

In the present paper, we describe the results of an experimental study of the production and thermal stability of Fe^{4+} ions in β-Ga_2O_3 crystals. Electron paramagnetic resonance (EPR), with its narrow linewidths and high sensitivity, is the primary spectroscopic technique used.[22–25] The Fe^{3+} ($3d^5$) ions in β-Ga_2O_3 crystals have a high spin S = 5/2 ground state with large zero-field splittings and suitable spin-lattice relaxation times, thus allowing them to be easily detected and identified with EPR.[26,27] In contrast, EPR spectra from the non-Kramers Fe^{2+} ($3d^6$) and Fe^{4+} ($3d^4$) ions have not yet been reported for β-Ga_2O_3.[28,29] We can, however, easily determine when Fe^{2+} and Fe^{4+} ions are present in our crystals by monitoring changes in the intensity of the Fe^{3+} EPR spectrum. We use 325 nm laser light to convert Fe^{3+} ions into Fe^{4+} and Fe^{2+} ions

in an Mg-doped β-Ga_2O_3 crystal that inadvertently contains a moderate concentration of iron. The recovery of the Fe^{3+} spectrum as a function of time, after removing the light, is recorded at five temperatures between 250 and 270 K. An activation energy describing the thermal excitation of electrons from the valence band to the Fe^{4+} ions, and thus a value for the $Fe^{4+/3+}$ donor level, is extracted from these Fe^{3+} isothermal recovery curves taken from the Mg-doped crystal. Our analysis yields a value of 0.70 eV for this activation energy. Results from an Fe-doped β-Ga_2O_3 crystal are also reported. The 325 nm laser light readily forms Fe^{4+} ions in the Fe-doped crystal, and a similar value for the $Fe^{4+/3+}$ level is obtained from the isothermal decay of these Fe^{4+} ions.

Our noncontact EPR method was recently used to determine the $Fe^{2+/3+}$ and $Mg^{0/-}$ acceptor levels in β-Ga_2O_3 crystals.[8,30] The (0/−) level of the Mg acceptor was found to be 0.65 eV above the maximum of the valence band by recording thermal decay curves of the neutral Mg acceptor (Mg^0_{Ga}) in the 240–260 K range, whereas the (2+/3+) acceptor level of the Fe ions was found to be 0.84 eV below the minimum of the conduction band by recording thermal recovery curves of the Fe^{3+} ions in the 296–310 K range. The temperature range of 250–270 K for measurements in our present study is between these two earlier temperature ranges, and thus an intermediate value of 0.70 eV above the valence band is a reasonable, and expected, result for the activation energy describing the (4+/3+) donor level of Fe in β-Ga_2O_3.

II. EXPERIMENTAL

Two bulk β-Ga_2O_3 crystals, both grown by the Czochralski method with iridium crucibles, were used in the present investigation.[31–35] The first, and primary, sample studied was an Mg-doped crystal grown at Northrop Grumman Synoptics (Charlotte, NC), with 0.20 mol. % of MgO added to the starting material. This crystal was also used in Refs. 30 and 32, where it was determined with EPR that the as-grown concentrations of Ir^{4+} ions and singly ionized Mg acceptors (Mg^-_{Ga}) were both 7.0×10^{18} cm^{-3} and the as-grown concentration of Fe^{3+} ions was 1.4×10^{17} cm^{-3}. Cr^{3+} ions are also seen in this crystal, but at a concentration approximately 25 times less than the Fe^{3+} concentration. By using EPR, we are able to determine the concentrations of specific charge states of the impurity ions, instead of the total concentration of an element. The second sample studied was an Fe-doped crystal obtained from Kyma Technologies (Raleigh, NC). Fe_2O_3 was added to the starting material, and the resulting Fe^{3+} concentration in the as-grown crystal[8] was approximately 2.5×10^{19} cm^{-3}. Dimensions of the Mg-doped crystal were $5.0 \times 1.4 \times 3.0$ mm^3 and dimensions of the Fe-doped crystal were $4.0 \times 0.37 \times 3.0$ mm^3.

The EPR data were taken with a Bruker EMX spectrometer operating near 9.39 GHz. An Oxford Instruments ESR-900 cryostat and ITC-503S controller held the crystal at a fixed temperature during an EPR measurement. Flowing nitrogen gas, obtained from a liquid nitrogen storage dewar, was used to cool the crystal (instead of the usual cold helium gas). A He–Cd laser (12 mW of cw output at 325 nm) converted Fe^{3+} ions into Fe^{4+} and Fe^{2+} ions. When monitoring the concentration of Fe^{3+} ions before, during, and after light, the spectrometer was operated in a kinetics mode (i.e., a time sweep with the magnetic field fixed at the peak of a line in the EPR spectrum).

III. PRODUCTION AND DECAY OF Fe^{4+} IONS

Figure 1 shows two EPR spectra from Fe^{3+} ions in our Mg-doped β-Ga_2O_3 crystal. The magnetic field is aligned along the crystal's *b* direction in the upper spectrum and near the *c* direction in the lower spectrum. These spectra were obtained at room temperature, with no incident laser light. The four dominant EPR lines at 166.4, 283.5, 586.2, and 1293.7 mT in the upper spectrum and the one dominant line near 152.9 mT in the lower spectrum are assigned to Fe^{3+} ions at sixfold Ga^{3+} sites.[26,27] These lines shift very little in position when the crystal is cooled to 250 K. The Fe^{3+} ($3d^5$) ions in β-Ga_2O_3 have a high-spin S = 5/2 ground state with large zero-field splittings resulting from the low-symmetry monoclinic crystal structure. These splittings are the separations between the three distinct energy levels (corresponding to the pairwise degenerate $M_S = \pm 1/2$, $\pm 3/2$, and $\pm 5/2$ spin states) when the magnetic field is zero.[36] For Fe^{3+} ions in β-Ga_2O_3, the zero-field splittings are much larger in energy than our 9.39 GHz microwave photons, thus explaining the lack of symmetry around g = 2.0 (i.e., 335 mT) in the spectra. Short spin-lattice relaxation times cause the EPR signal from Ir^{4+} ($5d^5$) ions to broaden beyond recognition when the temperature is above 120 K.[32] Although Ir^{4+} ions are present in the crystal,[30] they are not seen in the EPR spectra in Fig. 1. The infrared absorption peak at 5153 cm^{-1} from Ir^{4+} ions can, however, be easily observed at room temperature using a Fourier-transform infrared (FTIR) spectrometer.[32]

Figure 2 shows the intensity of the Fe^{3+} EPR spectrum before, during, and after exposure at 255 K to sub-bandgap 325 nm laser

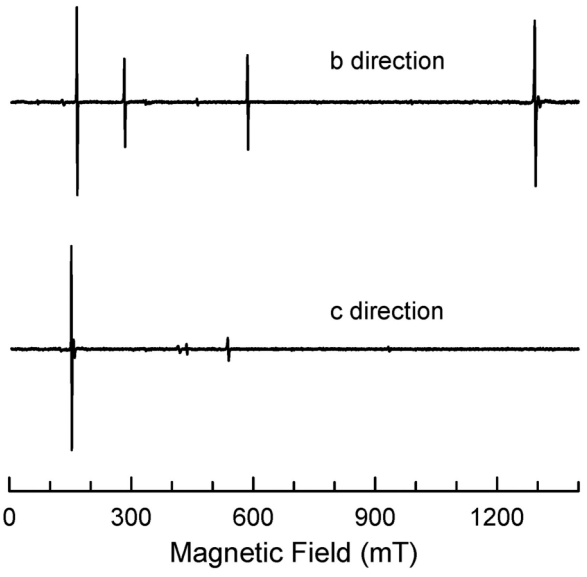

FIG. 1. EPR spectra from Fe^{3+} ions occupying sixfold Ga^{3+} sites in an Mg-doped β-Ga_2O_3 crystal. These data were taken at room temperature with a microwave frequency of 9.381 GHz. The magnetic field is aligned along the *b* axis of the crystal in the upper spectrum and near the *c* axis in the lower spectrum.

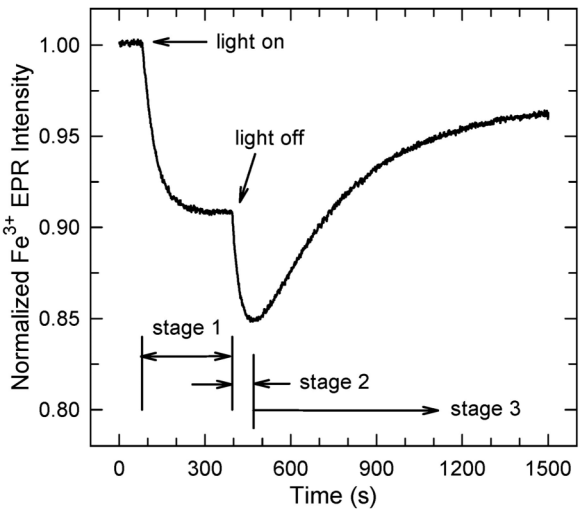

FIG. 2. Normalized intensity of the Fe^{3+} EPR spectrum in an Mg-doped β-Ga_2O_3 crystal before, during, and after exposure to 325 nm laser light. The magnetic field was near the *c* direction and fixed at 152.9 mT and the temperature was 255 K. At 80 s, the light is turned on and a decrease in the concentration of Fe^{3+} ions occurs. When the light is removed at 395 s, the Fe^{3+} ions have a further significant decrease before starting to recover near 470 s. The horizontal time axis is separated into three regions (stage 1, stage 2, and stage 3).

light. These data were obtained by monitoring the Fe^{3+} line located at 152.9 mT when the magnetic field is near the *c* direction (see Fig. 1). The changes in the intensity of the Fe^{3+} spectrum can be separated into three stages, as illustrated in Fig. 2. Different, but related, physical mechanisms (described in the following paragraphs) are active at each stage. With the light on (referred to as stage 1, from 80 to 395 s), the Fe^{3+} spectrum decreases and then reaches an equilibrium value. There is a 9% reduction in the concentration of Fe^{3+} ions during this phase. After the light is removed, the intensity of the Fe^{3+} spectrum continues to decrease for another 75 s (referred to as stage 2). Near the 470 s point in Fig. 2, the Fe^{3+} spectrum begins to slowly recover. This recovery is referred to as stage 3. The recovering Fe^{3+} EPR spectrum approaches a new equilibrium intensity beyond 1500 s, which is below the initial intensity observed before turning on the light.

In stage 1, the 325 nm light reduces the concentration of Fe^{3+} ions, as both Fe^{4+} and Fe^{2+} ions can, in principal, be formed. Three processes are involved in this phase. First, consider the formation of Fe^{4+} ions. The sub-bandgap 325 nm (3.81 eV) photons excite electrons from one or more of the valence bands to singly ionized Ir^{4+} donors, as described in Ref. 30. This mechanism for production of Ir^{3+} ions is consistent with the $Ir^{4+/3+}$ level being 2.25 eV below the conduction band minimum.[37] As electrons move to Ir^{4+} ions, many of the holes left in the valence band become localized at singly ionized Mg acceptors and form neutral acceptors (Mg^0_{Ga}). At the same time, and most important for the present study, a portion of these holes left in the valence band are trapped at Fe^{3+} ions and form Fe^{4+} ions. Second, consider the formation of Fe^{2+} ions during stage 1. In an earlier study of an Fe-doped β-Ga_2O_3 crystal, two mechanisms were proposed.[8] The 325 nm photons may excite electrons directly from the upper valence band to Fe^{3+} ions and they may also excite electrons from Ir^{3+} ions to the conduction band, with the electrons being subsequently trapped at Fe^{3+} ions in this latter case. Together, these processes form Fe^{2+} ions in our Mg-doped crystal that are very long-lived at 255 K. Since there are initially far fewer Fe^{3+} ions in this crystal than Ir^{4+} donors and singly ionized Mg acceptors, the 325 nm light produces more Fe^{4+} ions than Fe^{2+} ions in stage 1.

In stage 2, the decrease in the concentration of Fe^{3+} ions is directly related to the formation of even more Fe^{4+} ions, although this now occurs in the "dark." The neutral Mg acceptors formed with laser light during stage 1 quickly begin to thermally decay at 255 K when the light is removed.[30] Many of the holes produced in the upper valence band by these decaying Mg^0_{Ga} acceptors move to Ir^{3+} ions, but a portion of them move to Fe^{3+} ions and form more Fe^{4+} ions. The rate of decrease that occurs for the Fe^{3+} spectrum between 395 and 470 s in Fig. 2 (immediately after turning the light off) is very similar to the rate of decrease reported in Ref. 30 for the decay of Mg^0_{Ga} acceptors at 255 K. Near the 470 s point in Fig. 2, the Fe^{3+} spectrum begins to recover as the thermal decay of Fe^{4+} ions (due to electrons being thermally excited from the valence band to the Fe^{4+} ions) exceeds the production of Fe^{4+} ions caused by decaying Mg^0_{Ga} acceptors. As shown in Ref. 30, the thermal decay of the Mg^0_{Ga} acceptors is relatively fast at 255 K, with approximately 72% decaying in the first 100 s after removing the laser light. In Fig. 2, this continuing decrease in the Fe^{3+} concentration in stage 2, before starting to increase in stage 3, provides compelling evidence that Fe^{4+} ions are being formed. It also requires the $Mg^{0/-}$ level to be below the $Fe^{4+/3+}$ level.

In stage 3, which extends for a much longer time than stage 2, the primary active mechanism is the thermal decay of the Fe^{4+} ions. This slow recovery of the Fe^{3+} EPR signal in Fig. 2 occurs as electrons are thermally excited from the upper valence band to the Fe^{4+} ions. The concentration of Fe^{3+} ions eventually reaches a quasiequilibrium level when all the Fe^{4+} ions have thermally decayed. This equilibrium level occurs beyond 1500 s and is below the initial concentration of Fe^{3+} ions present before turning on the light. The difference in intensity of the Fe^{3+} spectrum at t = 0 and t = 1500 s in Fig. 2 is attributed to the small concentration of Fe^{2+} ions that are initially formed by the 325 nm light and remain relatively stable at 255 K. An activation energy of 0.84 eV for the thermal excitation of electrons from the Fe^{2+} ions to the conduction band[8] suggests that less than 0.4% of these ions would thermally decay over a 1400 s period at 255 K.

The EPR experiment illustrated in Fig. 2 was repeated at four additional temperatures, thus providing five sets of Fe^{3+} isothermal recovery data (at 250, 255, 260, 265, and 270 K) from the Mg-doped β-Ga_2O_3 crystal. The general features of the recovery curves were similar for all five temperatures. There was always a further decrease in the concentration of Fe^{3+} ions immediately after removing the light (corresponding to stage 2). These five sets of data are shown in Fig. 3. Our focus is on the thermal decay of the Fe^{4+} ions, and not the recovery of the Fe^{3+} ions, thus the curves in Fig. 3 have been inverted and normalized. The time when the laser light was turned off is now set to t = 0. Also, the offset due to the nearly constant Fe^{2+} contribution was removed from each curve

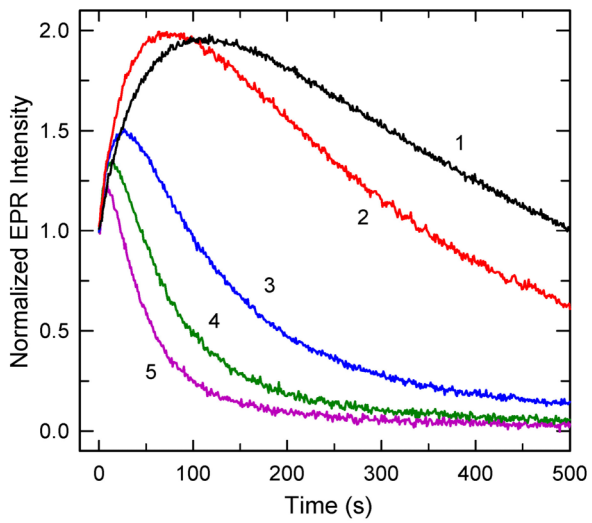

FIG. 3. Isothermal recovery curves for the Fe^{3+} EPR signal in an Mg-doped β-Ga_2O_3 crystal, taken at (1) 250, (2) 255, (3) 260, (4) 265, and (5) 270 K. These curves have been "inverted" to emphasize the behavior of the Fe^{4+} ions. They show the initial production of Fe^{4+} ions at short times (in stage 2) and the subsequent decay of the Fe^{4+} ions at longer times (in stage 3). Contributions from the very slowly decaying Fe^{2+} ions have been removed.

before normalizing at t = 0. This ensures that the curves in Fig. 3 represent only changes in the Fe^{4+} concentration. Prior to recording each isothermal curve, the crystal was heated briefly to 523 K to remove the effects of previous illuminations and reset the thermal equilibrium concentrations of Fe^{3+} and Ir^{4+} ions.

IV. ANALYSIS OF Fe^{4+} THERMAL DECAY CURVES

The thermal release of charge trapped in metastable states within the bandgap of materials has long been studied by the thermoluminescence community.[38–40] Several general approaches to analyze decay data have emerged from these efforts, with the choice of method depending on the procedure used to acquire data and also the types of participating traps and recombination centers, their nature, and their relative concentrations. The extent to which thermally released charge is retrapped is often an important factor in selecting a model. A general-order kinetics model[41] was used in the recent EPR determinations of $Fe^{2+/3+}$ and $Mg^{0/-}$ levels in β-Ga_2O_3 crystals.[8,30] During the isothermal decays in those studies, there was significant retrapping of charge at the same defect involved in the thermal release of the charge. In the present investigation, the Fe^{4+} decay curves taken from the Mg-doped crystal (in Sec. III) are analyzed using a simpler first-order kinetics model.[42] Only the data obtained in stage 3, after nearly all the Mg^0_{Ga} acceptors have decayed, are considered. At these longer times, retrapping of holes at Fe ions is negligible, thus justifying the use of first-order kinetics. Specifically, when electrons are thermally excited from the valence band to an Fe^{4+} ion during stage 3, most of the holes left behind do not move to Fe^{3+} ions and re-establish Fe^{4+} ions. Instead, these holes are attracted to the negatively charged singly ionized Mg acceptors (Mg^-_{Ga}). They may be trapped, released, and retrapped several times at these acceptors before finally making their way to an Ir^{3+} ion or an Fe^{2+} ion, but this series of events has very little effect on the rate of decay of the Fe^{4+} ions. The lack of retrapping of holes at Fe^{3+} ions in our Mg-doped crystal, during an isothermal kinetic scan, is primarily a result of the concentration of Fe ions being much less than the concentration of Mg and Ir ions.

The following equation defines the first-order kinetics model used to extract an activation energy from the Fe^{4+} isothermal decay curves,

$$\frac{dn}{dt} = -s\,n\exp(-E/kT). \tag{1}$$

Here, n is the concentration of Fe^{4+} ions, E is the activation energy, k is Boltzmann's constant, T is the temperature, and s is a fitting parameter often referred to as an "attempt-to-escape" frequency. The solution of Eq. (1), given below, is a single exponential that describes the decreasing concentration of Fe^{4+} ions as a function of time for a fixed temperature,

$$n(t) = n_0\exp[-s\exp(-E/kT)t]. \tag{2}$$

A characteristic feature of a first-order kinetics process is a straight line when the natural logarithm of n(t) is plotted vs t. To illustrate this, take the natural logarithm of both sides of Eq. (2),

$$\ln(n) = \ln(n_0) - s\exp(-E/kT)t. \tag{3}$$

Equation (3) has the form of a straight line (y = a − mt), where the slope is

$$m = s\exp(-E/kT). \tag{4}$$

The Fe^{4+} decay data taken at 250 K (curve 1 in Fig. 3) are converted into a plot of ln(n) vs t in Fig. 4. As shown in this figure, a straight line (red) is a good fit to the region extending from 300 to 1400 s. This restricted time interval for extracting a straight line avoids the early times when the decaying neutral Mg acceptors may still be forming Fe^{4+} ions. The longest times are avoided because of the uncertainty associated with removing the small contributions from Fe^{2+} ions (this removal was done when generating the 250 K curve in Fig. 3). Most of the Fe^{4+} decay is captured in the selected time interval. Figure 4 also shows the plots of ln(n)-vs-t generated using the Fe^{4+} decay data (in Fig. 3) taken at 255, 260, 265, and 270 K. The segments of time used to extract a straight line were 225 to 850 s for 255 K, 60 to 210 s for 260 K, 35 to 150 s for 265 K, and 20 to 75 s for 270 K. These time intervals are progressively smaller at the higher temperatures because of the faster decay rates of the Fe^{4+} ions. Each ln(n)-vs-t plot in Fig. 4 yields a straight line (with a different slope) in the selected time intervals, thus validating the use of a first-order kinetics model.

To extract values for E and s from the Fe^{4+} ion isothermal decay data, we take the natural logarithm of each side of Eq. (4).

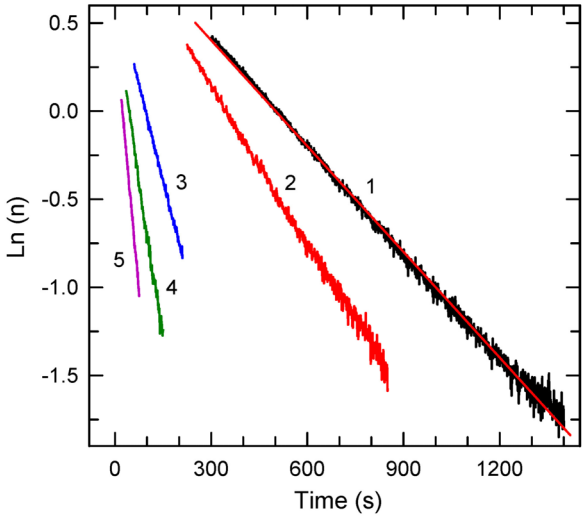

FIG. 4. Plots of ln(n) vs t for the isothermal decay of Fe^{4+} ions at (1) 250, (2) 255, (3) 260, (4) 265, and (5) 270 K in an Mg-doped β-Ga_2O_3 crystal. As predicted by first-order kinetics, these plots are very close to straight lines for the chosen time intervals. This is illustrated by the best-fit straight line (red) plotted on top of the 250 K data.

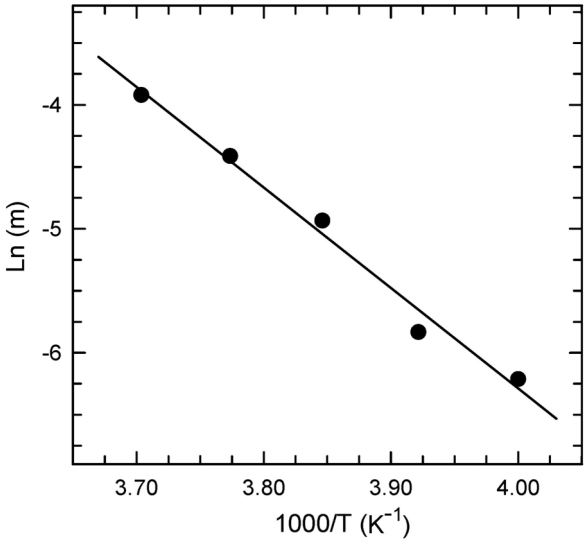

FIG. 5. A plot of $\ln(m_i)$ vs $1/T_i$ for the five temperatures where Fe^{4+} decay data were recorded. The slope (−E/k) of the "best-fit" straight line gives a value of 0.70 eV for the activation energy describing the thermal decay of Fe^{4+} ions in β-Ga_2O_3.

This gives

$$\ln(m_i) = \ln(s) - \frac{E}{kT_i}. \quad (5)$$

The index i = 1 to 5 corresponds to the five temperatures where decay data were obtained. Using the values of m_i obtained from the ln(n)-vs-t plots in Fig. 4, we construct the $\ln(m_i)$-vs-$1/T_i$ plot that is shown in Fig. 5. According to Eq. (5), these five data points will lie on a straight line with a slope of –E/k. The slope of the best-fit straight line in Fig. 5 gives E = 0.70 eV for the activation energy describing the thermal decay of photoinduced Fe^{4+} ions in β-Ga_2O_3 crystals. An estimate of the uncertainty in this value of E is ±0.05 eV. Our experimental result of 0.70 eV above the valence band maximum for the $Fe^{4+/3+}$ donor level is close to the recent computational prediction of 0.51 eV.[2,7] The vertical-axis intercept in Fig. 5 gives a value of $2.3 \times 10^{11}\ s^{-1}$ for the attempt-to-escape frequency s. This is a typical result for thermally stimulated processes, and s is often associated with the frequencies of lattice vibrations (i.e., phonons).[38–40]

V. Fe^{4+} IONS IN Fe-DOPED CRYSTALS

The intensity of the sixfold Fe^{3+} EPR spectrum in an Fe-doped β-Ga_2O_3 crystal was monitored before, during, and after exposure to sub-bandgap 325 nm laser light. These results, obtained while the crystal was held at 255 K, are shown in Fig. 6. This kinetic scan was taken with the magnetic field aligned near the *c* direction and fixed at 152.9 mT. Approximately 35% of the Fe^{3+} ions are converted to other charge states (Fe^{2+} and Fe^{4+}) by the light. The data in Fig. 6 were obtained from the Fe-doped crystal that was used in Ref. 8. In that earlier study,[8] the two mechanisms proposed for the formation of Fe^{2+} ions by the 325 nm light were (1) excitation of electrons from Ir^{3+} ions to the conduction band followed by trapping of these electrons by Fe^{3+} ions to form Fe^{2+}

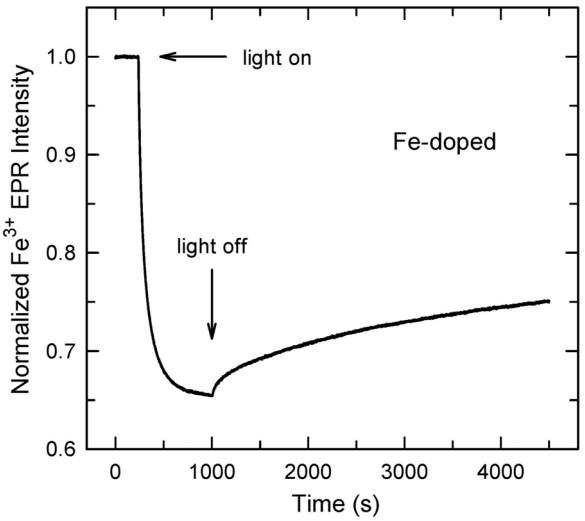

FIG. 6. Normalized intensity of the Fe^{3+} EPR spectrum in an Fe-doped β-Ga_2O_3 crystal before, during, and after exposure to 325 nm laser light. The temperature was 255 K and the magnetic field, near the *c* direction, was fixed at 152.9 mT. At 236 s, the light is turned on and a decrease in the concentration of Fe^{3+} ions is seen, as Fe^{2+} and Fe^{4+} ions are formed. When the light is removed at 1000 s, the concentration of Fe^{3+} ions immediately begins to recover.

ions and (2) excitation of electrons from the upper valence band to the Fe^{3+} ions with the holes left in the valence band being trapped on Ir^{3+} ions and forming Ir^{4+} ions. The formation of Fe^{4+} ions in the Fe-doped crystal may also occur during mechanism 2. After excitation of electrons from the valence band to the Fe^{3+} ions, a portion of the holes left in the valence band will be trapped at other Fe^{3+} ions and form Fe^{4+} ions (as well as being trapped at Ir^{3+} ions and forming Ir^{4+} ions). In Sec. III of the present paper, the mechanism suggested for the formation of Fe^{4+} ions in the Mg-doped crystal involves excitation of electrons from the valence band to Ir^{4+} ions with the holes left in the valence band being trapped as Fe^{4+} ions. However, this Fe^{4+} formation process in the Mg-doped crystal is not expected to dominate in the Fe-doped crystal, as there are very few Ir^{4+} ions (only Ir^{3+} ions) in the Fe-doped crystal before exposure to the 325 nm light.

The temperature where EPR data are taken is an important distinction between the present work and the earlier study of the $Fe^{2+/3+}$ level.[8] In Ref. 8, the isothermal recovery curves for Fe^{3+} ions in the Fe-doped crystal were taken at temperatures near or slightly above room temperature, whereas the recovery curve in Fig. 6 was taken at 255 K. Our present results from the Mg-doped crystal (in Sec. IV) indicate that any Fe^{4+} ions formed with light at 296 K in the earlier study[8] would have thermally decayed in 20 s or less when the light was removed, and would not have affected the Fe^{3+} recovery curves that extended over several 1000s of seconds. Thus, information about the $Fe^{4+/3+}$ level was not extracted from the Fe^{3+} recovery curves taken between 296 and 310 K in Ref. 8. We also note that the trace levels of Cr^{3+} ions in our Fe-doped crystal do not play a significant role in the photoinduced decrease and subsequent isothermal recovery of Fe^{3+} ions at either 255 K or near room temperature (the concentration of Cr is much smaller than the concentration of Fe). The Cr^{3+} ions provided important information in Ref. 8 about the recombination process monitored by thermoluminescence (TL) and photoluminescence (PL). Because of the highly efficient nature of their emission near 700 nm, only a very small number of Cr^{3+} ions were needed to produce observable PL and TL peaks.

In our present study, the behavior reported as stage 2 in the Mg-doped crystal (i.e., the further decrease of Fe^{3+} ions after removal of the light in Fig. 2) is not present in Fig. 6 since there are very few Mg acceptors in this Fe-doped crystal. Instead, the Fe^{3+} spectrum immediately begins to recover when the light is removed. As previously described for the Mg-doped crystal, the recovery occurs when Fe^{4+} ions are converted to Fe^{3+} ions by electrons thermally excited from the valence band. At the longer times in Fig. 6, the recovering Fe^{3+} EPR spectrum slowly approaches an equilibrium level below the initial "before light" intensity. The more stable Fe^{2+} ions initially formed by the light are responsible for this portion of Fe^{3+} ions that have not yet recovered (as described in Ref. 8, these Fe^{2+} ions will convert to Fe^{3+} if the crystal is warmed to near or above room temperature). At 255 K, it is clear from Fig. 6 that the 325 nm light produces more Fe^{2+} ions than Fe^{4+} ions in the Fe-doped crystal. This is opposite the behavior observed at 255 K in the Mg-doped crystal (see Fig. 2), where the light produces more Fe^{4+} ions than Fe^{2+} ions.

The amount of recovery of the Fe^{3+} signal in Fig. 6 (after removing the light) provides evidence that Fe^{4+} ions are being formed in the Fe-doped crystal. If only Fe^{2+} ions are produced during the exposure to light, then the subsequent recovery of the Fe^{3+} signal after removing the light should be a very small portion of the initial change generated by the light. The results in Ref. 8 predict that slightly less than 1% of the Fe^{2+} ions produced by the light will decay at 255 K during the first 3500 s after removing the light. As is seen in Fig. 6, the actual amount of recovery of the Fe^{3+} ions during this time interval is 30% of the initial photoinduced decrease. We thus conclude that the recovery of Fe^{3+} ions at 255 K, after removing the light, is primarily caused by the thermal decay of Fe^{4+} ions.

An approximate value for the $Fe^{4+/3+}$ level is obtained from the Fe^{3+} recovery data taken at 255 K from the Fe-doped crystal. As a first step, the recovery data in Fig. 6 are inverted and normalized, and then replotted in Fig. 7, with t = 0 chosen to be when the laser light was turned off. The normalization process uses the difference between the intensity of the Fe^{3+} signal before turning on the light and its intensity just before turning off the light. When performing the normalization, the following small adjustment was also included. As shown in the inset to Fig. 7, the rate of recovery of the Fe^{3+} ions during the first 200 s is faster than at the later times, thus indicating that a secondary mechanism is active during this brief period. This initial fast change is attributed to donor–acceptor recombination involving a small concentration of close pairs of Ir^{4+}-Fe^{2+} and Fe^{4+}–Fe^{2+} ions, driven by the overlap of their wave functions and not requiring the release of charge to the conduction or valence band. To remove this direct recombination effect from the decay data in Fig. 7, the intensity used in the normalization process (at t = 0) was set at a value 5% lower than the actual

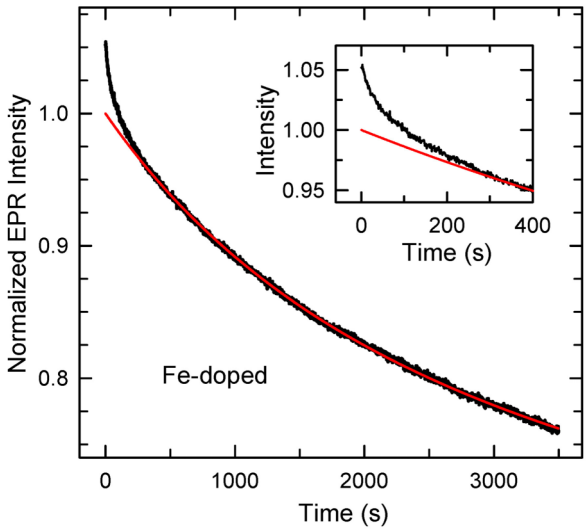

FIG. 7. An isothermal recovery curve for the Fe^{3+} EPR signal in an Fe-doped β-Ga_2O_3 crystal, acquired at 255 K. These data, taken from Fig. 6, have been "inverted" to emphasize the decay of the Fe^{4+} ions. The solid (red) line was generated using the best-fit parameters obtained from the general-order kinetics model. The inset shows the faster rate of recovery of the Fe^{3+} signal during the first 200 s after removing the light.

intensity (see the inset). After the first 200 s, these data in Fig 7 describe the thermal decay of isolated Fe^{4+} ions.

When compared to the 255 K results from the Mg-doped crystal in Fig. 2, the decay of the Fe^{4+} ions in Fig. 7 is much slower. This indicates that there is significant retrapping of holes at Fe^{3+} ions (and thus reforming of Fe^{4+} ions). The increased retrapping in the Fe-doped crystal is caused by the larger number of Fe^{3+} ions and a lack of Mg acceptors. The following general-order kinetics model, with b near 2, is used to extract a value for the $Fe^{4+/3+}$ level from the data in Fig. 7,

$$\frac{dn}{dt} = -s' n^b \exp(-E/kT). \quad (6)$$

This is the same general-order kinetics approach used to determine the $Fe^{2+/3+}$ level in the Fe-doped β-Ga_2O_3 crystal.[8] The solution to Eq. (6), for $b > 1$, is

$$n(t) = n_0[1 + s' n_0^{b-1}(b-1)\exp(-E/kT)t]^{\frac{1}{1-b}}. \quad (7)$$

Equation (7) is rewritten in the following form with the parameter x included to account for the fractional portion of Fe^{2+} ions produced by the light,

$$\frac{n}{n_0} = (1-x)(1+a\,t)^c + x. \quad (8)$$

Here, $a = s' n_0^{b-1}(b-1)\exp(-E/kT)$. and $c = (1-b)^{-1}$. Choosing the order parameter b to be 1.9 (representing a high degree of retrapping), the data in Fig. 7 are then fitted using Eq. (8) with a and x being the variables. The best-fit values are $a = 2.89 \times 10^{-4}$ and $x = 0.56$. This value for x indicates that 56% of the initial photoinduced decrease of Fe^{3+} ions is due to the formation of the more stable Fe^{2+} ions. The solid line (red) in Fig. 7, generated with these values for a and x, is in good agreement with the data. Substituting T = 255 K, b = 1.9, and $s' n_0^{b-1} = 9.5 \times 10^{10}\ s^{-1}$ into the expression for a and then solving for E gives 0.73 eV for the $Fe^{4+/3+}$ level. The value we are using for $s' n_0^{b-1}$ is taken from Ref. 8, where this same Fe-doped crystal was used to determine the $Fe^{2+/3+}$ level. Our approximate result of 0.73 eV for E obtained from the Fe-doped crystal is close to the value of 0.70 eV obtained from the more comprehensive analysis in Sec. IV using data from the Mg-doped crystal.

VI. SUMMARY

The electron paramagnetic resonance (EPR) spectrum from Fe^{3+} ions is used to monitor the production and thermal decay of Fe^{4+} ions in a bulk Mg-doped β-Ga_2O_3 crystal. For temperatures in the 250–270 K range, a 325 nm laser converts Fe^{3+} ions to Fe^{4+} ions (and a smaller number of Fe^{2+} ions) and also produces neutral Mg acceptors (Mg_{Ga}^0) and deep neutral iridium donors (Ir^{3+}). When the light is removed, the quick decay at these temperatures of the less stable Mg_{Ga}^0 acceptors causes a further drop in the concentration of Fe^{3+} ions. This unique isothermal post-light decrease provides direct evidence that Fe^{4+} ions are being formed in the crystal. Following these production steps, the initial (pre-light) concentration of Fe^{3+} ions is slowly restored in the 250–270 K temperature range as electrons are thermally excited to Fe^{4+} ions from the valence band. A first-order kinetics model (with minimal retrapping) describes the experimental results and is used to extract an activation energy, and thus a value for the $Fe^{4+/3+}$ level. Our analysis, using five isothermal decay curves taken from the Mg-doped crystal, places the $Fe^{4+/3+}$ level 0.70 eV (±0.05 eV) above the valence band maximum in β-Ga_2O_3.

We also show with EPR that Fe^{4+} ions can be produced with 325 nm light in an Fe-doped β-Ga_2O_3 crystal. Because of the much larger concentration of Fe, there is significantly more retrapping of holes at Fe^{3+} ions during the thermal decay of these Fe^{4+} ions. This results in a noticeably slower decay of the Fe^{4+} ions when compared to the Mg-doped crystal. A simple, yet informative, examination of the Fe^{3+} recovery data taken at 255 K from the Fe-doped crystal gives an approximate value of 0.73 eV above the valence band maximum for the $Fe^{4+/3+}$ level.

An important result from our study is the requirement that the $Mg^{0/-}$ acceptor level be closer to the valence band than the $Fe^{4+/3+}$ donor level. Computational studies have, thus far, predicted a reverse order for these levels. Having the $Fe^{4+/3+}$ donor level farther from the valence band than the $Mg^{0/-}$ acceptor level suggests that Fe impurities can play a role in compensation of Mg acceptors (and other shallower acceptors) in β-Ga_2O_3 crystals (e.g., when growth techniques are used that do not introduce iridium donors). This acceptor-compensating role of Fe may be a further impediment to producing *p*-type β-Ga_2O_3, especially when Fe doped semi-insulating substrates are used to grow thin films.

ACKNOWLEDGMENTS

The present work was funded in part by the Air Force Office of Scientific Research under Award No. F4FGA08054J003. One of the authors (T.D.G.) was supported at the Air Force Institute of Technology by an NRC Research Associateship Award. Any opinions, findings, and conclusions or recommendations expressed in this paper are those of the authors and do not necessarily reflect the views of the United States Air Force.

DATA AVAILABILITY

The data that support the findings of this study are available within the article.

REFERENCES

[1]M. D. McCluskey, "Point defects in Ga_2O_3," J. Appl. Phys. **127**, 101101 (2020).
[2]M. E. Ingebrigtsen, J. B. Varley, A. Y. Kuznetsov, B. G. Svensson, G. Alfieri, A. Mihaila, U. Badstübner, and L. Vines, "Iron and intrinsic deep level states in Ga_2O_3," Appl. Phys. Lett. **112**, 042104 (2018).
[3]A. T. Neal, S. Mou, S. Rafique, H. Zhao, E. Ahmadi, J. S. Speck, K. T. Stevens, J. D. Blevins, D. B. Thomson, N. Moser, K. D. Chabak, and G. H. Jessen, "Donors and deep acceptors in β-Ga_2O_3," Appl. Phys. Lett. **113**, 062101 (2018).
[4]A. Y. Polyakov, N. B. Smirnov, I. V. Shchemerov, S. J. Pearton, F. Ren, A. V. Chernykh, and A. I. Kochkova, "Electrical properties of bulk semi-insulating β-Ga_2O_3 (Fe)," Appl. Phys. Lett. **113**, 142102 (2018).
[5]A. Y. Polyakov, N. B. Smirnov, I. V. Schemerov, A. V. Chernykh, E. B. Yakimov, A. I. Kochkova, A. N. Tereshchenko, and S. J. Pearton, "Electrical

properties, deep levels and luminescence related to Fe in bulk semi-insulating β-Ga_2O_3 doped with Fe," ECS J. Solid State Sci. Technol. **8**, Q3091 (2019).
[6]C. Joishi, Z. Xia, J. McGlone, Y. Zhang, A. R. Arehart, S. Ringel, S. Lodha, and S. Rajan, "Effect of buffer iron doping on delta-doped β-Ga_2O_3 metal semiconductor field effect transistors," Appl. Phys. Lett. **113**, 123501 (2018).
[7]S. Bhandari, M. E. Zvanut, and J. B. Varley, "Optical absorption of Fe in doped Ga_2O_3," J. Appl. Phys. **126**, 165703 (2019).
[8]C. A. Lenyk, T. D. Gustafson, L. E. Halliburton, and N. C. Giles, "Deep donors and acceptors in β-Ga_2O_3 crystals: Determination of the $Fe^{2+/3+}$ level by a noncontact method," J. Appl. Phys. **126**, 245701 (2019).
[9]I. Hany, G. Yang, C. E. Zhou, C. Sun, K. Gundogdu, D. Seyitliyev, E. O. Danilov, F. N. Castellano, D. Sun, and E. Vetter, "Low temperature cathodoluminescence study of Fe-doped β-Ga_2O_3," Mater. Lett. **257**, 126744 (2019).
[10]S. Bhandari and M. E. Zvanut, "Optical transitions for impurities in Ga_2O_3 as determined by photoinduced electron paramagnetic resonance spectroscopy," J. Appl. Phys. **127**, 065704 (2020).
[11]Y. Tomioka, Y. Ozaki, H. Inaba, and T. Ito, "Compensation effects between impurity cations in single crystals of a wide gap semiconductor β-Ga_2O_3 prepared by the floating zone method," Jpn. J. Appl. Phys. **58**, 091009 (2019).
[12]B. Mallesham, S. Roy, S. Bose, A. N. Nair, S. Sreenivasan, V. Shutthanandan, and C. V. Ramana, "Crystal chemistry, band-gap red shift, and electrocatalytic activity of iron-doped gallium oxide ceramics," ACS Omega **5**, 104 (2020).
[13]C. Zimmermann, Y. K. Frodason, A. W. Barnard, J. B. Varley, K. Irmscher, Z. Galazka, A. Karjalainen, W. E. Meyer, F. D. Auret, and L. Vines, "Ti- and Fe-related charge transition levels in β-Ga_2O_3," Appl. Phys. Lett. **116**, 072101 (2020).
[14]A. Y. Polyakov, N. B. Smirnov, I. V. Shchemerov, A. Vasilev, E. B. Yakimov, A. V. Chernykh, A. I. Kochkova, P. B. Lagov, Y. S. Pavlov, O. F. Kukharchuk, A. A. Suvorov, N. S. Garanin, I.-H. Lee, M. Xian, F. Ren, and S. J. Pearton, "Pulsed fast reactor neutron irradiation effects in Si-doped n-type β-Ga_2O_3," J. Phys. D Appl. Phys. **53**, 274001 (2020).
[15]A. Y. Polyakov, I.-H. Lee, N. B. Smirnov, I. V. Shchemerov, A. A. Vasilev, A. V. Chernykh, and S. J. Pearton, "Electric field dependence of major electron trap emission in bulk β-Ga_2O_3: Poole-Frenkel effect versus phonon-assisted tunneling," J. Phys. D Appl. Phys. **53**, 304001 (2020).
[16]A. Y. Polyakov, I.-H. Lee, A. Miakonkikh, A. V. Chernykh, N. B. Smirnov, I. V. Shchemerov, A. I. Kochkova, A. A. Vasilev, and S. J. Pearton, "Anisotropy of hydrogen plasma effects in bulk n-type β-Ga_2O_3," J. Appl. Phys. **127**, 175702 (2020).
[17]C. Zimmermann, Y. K. Frodason, V. Rønning, J. B. Varley, and L. Vines, "Combining steady-state photo-capacitance spectra with first-principles calculations: The case of Fe and Ti in β-Ga_2O_3," New J. Phys. **22**, 063033 (2020).
[18]I. Hany, G. Yang, and C.-C. Chung, "Fast x-ray detectors based on bulk β-Ga_2O_3 (Fe)," J. Mater. Sci. **55**, 9461 (2020).
[19]H. Zhang, H.-L. Tang, N.-T. He, Z.-C. Zhu, J.-W. Chen, B. Liu, and J. Xu, "Growth and physical characterization of high resistivity Fe: B-Ga_2O_3 crystals," Chin. Phys. B **29**, 087201 (2020).
[20]M. H. Wong, K. Sasaki, A. Kuramata, S. Yamakoshi, and M. Higashiwaki, "Anomalous Fe diffusion in Si-ion-implanted β-Ga_2O_3 and its suppression in Ga_2O_3 transistor structures through highly resistive buffer layers," Appl. Phys. Lett. **106**, 032105 (2015).
[21]A. Alkauskas, M. D. McCluskey, and C. G. Van de Walle, "Tutorial: Defects in semiconductors—Combining experiment and theory," J. Appl. Phys. **119**, 181101 (2016).
[22]A. Abragam and B. Bleaney, *Electron Paramagnetic Resonance of Transition Ions* (Oxford University Press, London, 1970).
[23]J.-M. Spaeth and H. Overhof, *Point Defects in Semiconductors and Insulators Determination of Atomic and Electronic Structure From Paramagnetic Hyperfine Interactions* (Springer-Verlag, Berlin, 2003).
[24]J. A. Weil and J. R. Bolton, *Electron Paramagnetic Resonance: Elementary Theory and Practical Applications*, 2nd ed. (John Wiley and Sons, Hoboken, NJ, 2007).
[25]A. van der Est, "Continuous-wave EPR," in *EPR Spectroscopy: Fundamentals and Methods*, edited by D. Goldfarb and S. Stoll (John Wiley & Sons, Chichester, 2018), Chap. 1.
[26]M. L. Meilman, "EPR of Fe^{3+} ions in β-Ga_2O_3 crystals," Sov. Phys. Solid State **11**, 1403 (1969).
[27]R. Büscher and G. Lehmann, "Correlation of zero-field splittings and site distortions. IX. Fe^{3+} and Cr^{3+} in β-Ga_2O_3," Z. Naturforsch. **42a**, 67 (1987).
[28]M. A. Brown, "Measurements of the thermal conductivity of "pure" Al_2O_3 and $A1_2O_3$: Mg-possible observation of Fe^{4+} in Al_2O_3," J. Phys. C Solid State Phys. **6**, 642 (1973).
[29]R. T. Cox, "ESR of an *S*=2 centre in amethyst quartz and its possible identification as the d^4 ion Fe^{4+}," J. Phys. C Solid State Phys. **9**, 3355 (1976).
[30]C. A. Lenyk, T. D. Gustafson, S. A. Basun, L. E. Halliburton, and N. C. Giles, "Experimental determination of the (0/−) level for Mg acceptors in β-Ga_2O_3 crystals," Appl. Phys. Lett. **116**, 142101 (2020).
[31]J. D. Blevins, K. Stevens, A. Lindsey, G. Foundos, and L. Sande, "Development of large diameter semi-insulating gallium oxide (Ga_2O_3) substrates," IEEE Trans. Semicond. Manuf. **32**, 466 (2019).
[32]C. A. Lenyk, N. C. Giles, E. M. Scherrer, B. E. Kananen, L. E. Halliburton, K. T. Stevens, G. K. Foundos, J. D. Blevins, D. L. Dorsey, and S. Mou, "Ir^{4+} ions in β-Ga_2O_3 crystals: An unintentional deep donor," J. Appl. Phys. **125**, 045703 (2019).
[33]M. Baldini, Z. Galazka, and G. Wagner, "Recent progress in the growth of β-Ga_2O_3 for power electronics applications," Mater. Sci. Semicond. Process. **78**, 132 (2018).
[34]Z. Galazka, R. Uecker, D. Klimm, K. Irmscher, M. Naumann, M. Pietsch, A. Kwasniewski, R. Bertram, S. Ganschow, and M. Bickermann, "Scaling-up of bulk β-Ga_2O_3 single crystals by the Czochralski method," ECS J. Solid State Sci. Technol. **6**, Q3007 (2017).
[35]Z. Galazka, K. Irmscher, R. Uecker, R. Bertram, M. Pietsch, A. Kwasniewski, M. Naumann, T. Schulz, R. Schewski, D. Klimm, and M. Bickermann, "On the bulk β-Ga_2O_3 single crystals grown by the Czochralski method," J. Cryst. Growth **404**, 184 (2014).
[36]J. Telser, "EPR interactions – zero-field splittings," in *EPR Spectroscopy: Fundamentals and Methods*, edited by D. Goldfarb and S. Stoll (John Wiley & Sons, Chichester, 2018), Chap. 3.
[37]J. R. Ritter, K. G. Lynn, and M. D. McCluskey, "Iridium-related complexes in Czochralski-grown β-Ga_2O_3," J. Appl. Phys. **126**, 225705 (2019).
[38]S. W. S. McKeever, *Thermoluminescence of Solids* (Cambridge University Press, Cambridge, Great Britain, 1985).
[39]R. Chen and S. W. S. McKeever, *Theory of Thermoluminescence and Related Phenomena* (World Scientific Publishing Co, Singapore, 1997).
[40]C. Furetta, *Handbook of Thermoluminescence*, 2nd ed. (World Scientific Publishing Co, Singapore, 2010).
[41]R. Chen, "Glow curves with general order kinetics," J. Electrochem. Soc. **116**, 1254 (1969).
[42]J. T. Randall and M. H. F. Wilkins, "Phosphorescence and electron traps. II. The interpretation of long-period phosphorescence," Proc. R. Soc. Lond. Ser. A **184**, 390 (1945).